Progress In Electromagnetics Research, Vol. 132, 113–128, 2012

DOUBLE PERIODIC COMPOSITE RIGHT/LEFT HANDED TRANSMISSION LINE BASED LEAKY WAVE ANTENNA BY SINGULAR PERTURBATION METHOD

M. Mujumdar*, C. Jin, and A. Alphones

School of Electrical and Electronic Engineering, Nanyang Technological University, Singapore 639798, Singapore

Abstract—The paper proposes a Composite Right/Left Handed double periodic transmission line structure with both inductance and capacitance loaded. The structure exhibits leaky wave radiation and hence can be considered for leaky wave antenna (LWA) applications. We have theoretically obtained dispersion characteristics using Singular perturbation method. Also, the radiation efficiency has been obtained for different modulation indices. A novel leaky wave radiation has been obtained below the left handed passband with narrow bandwidth. The proposed structure has been fabricated on FR4 substrate and measured. The simulated and measured results seem to be in good agreement.

1. INTRODUCTION

Composite Right/Left transmission lines (TLs) have attracted a lot of research interest in recent years. Their adaptation for leaky wave radiation has been under study by many research groups. Certain unique radiation properties may be obtained with composite right/left handed (CRLH) structures due to their unusual propagation characteristics. CRLH TL when employed as a leaky wave antenna provides the advantage of compact size along with both backward and forward radiation [1]. In this paper, we propose a TL whose inductances and capacitances have been loaded in a double periodic manner. Attempt has been made to analyse the proposed TL using single perturbation procedure. It has been found that there exists a leaky wave below the left handed (LH) passband for the double periodic TLs.

Received 11 July 2012, Accepted 27 August 2012, Scheduled 24 September 2012

* Corresponding author: Manisha D. Mujumdar (manisha1@e.ntu.edu.sg).

We provide an analysis for determining the propagation behaviour and dispersion characteristics of the proposed double periodic TL. Instead of going in for the conventional transmission line theory, Floquet theorem and the equivalent circuit approach, we use singular perturbation analysis. For conventional methods the nature of mode of propagation is considered to be a pure transverse electromagnetic (TEM) mode and the TL characteristics are calculated from the electrostatic capacitance of the TLs. But, we need to take into consideration the hybrid nature of the mode of propagation. In case of microstrip, the hybrid modes cannot be completely described in terms of static inductances and capacitances only [2]. The power density distributions of the symmetric electric component are almost similar to the transverse magnetic (TM) mode and hence we consider TM mode dispersion here to determine the propagation constant.

The singular perturbation procedure provides a better physical insight of the analysis. It starts with the exact solution of a related problem, then it uses mathematical methods to find an approximate solution to a problem which cannot be solved exactly by full wave analysis. Perturbation method provides an expression for the desired solution in terms of a formal power series in a parameter that quantifies the deviation from the exactly solvable problem. This parameter can be expressed and expanded as a series which will be an approximation to the full solution. The expression is given as $H = \delta^0 H_0 + \delta^1 H_1 + \delta^2 H_2 + \ldots + \delta^n H_n$ where δ is the depth of modulation [3].

Here H_0 represents the known solution to the exactly solvable initial problem, and $H_1, H_2, \ldots, H_n$ represent the higher-order terms which may be found iteratively by some systematic procedure. It is noted that in addition to the dispersion characteristic derived from the zeroth-order problem, the perturbation method also gives information about the radiation efficiency and the radiation angle for the optimum radiation efficiency, which are derived from the first-order and second-order problem. The flow chart of the singular perturbation procedure for the analysis of the periodic structure is shown in Fig. 2.

2. SINGULAR PERTURBATION ANALYSIS

The layouts of the double periodic TLs investigated are shown in Fig. 1. Singular perturbation method has been used to analyze the dispersion characteristics and the radiation efficiency of the compact LWAs and they are numerically estimated as a function of the frequency and the antenna length, respectively [3]. Also, the radiation angle has been estimated at the novel leaky-wave region. Single periodic CRLH TL structures have an equivalent circuit comprising of inductances and

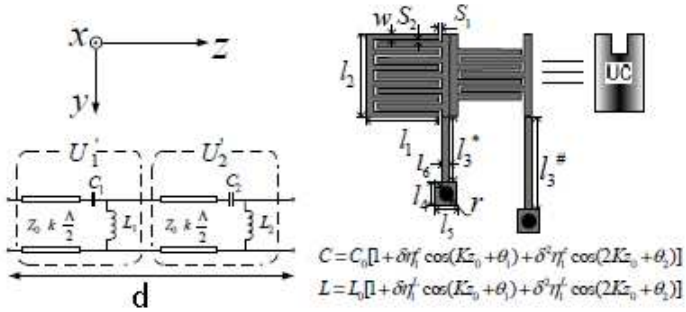

Figure 1. Layouts of the periodic TLs. (a) Model of unit cell of double periodic TLs. (b) Double periodic TL with different capacitances and inductances loaded. Substrate: $\varepsilon_r = 4.5$, thickness = 1.6 mm. $l_1 = 4.35$, $l_2 = 3.7$, $l_3^* = 4.5$, $l_3^\# = 7.9$, $l_4 = 1$, $l_5 = 1$, $l_6 = 0.5$, $S_1 = 0.15$, $S_2 = 0.15$, $w = 0.2$, $d = 5$. All are in mm.

capacitances.

The effective permeability and permittivity in double periodic TLs can be represented by the series inductance $L_R = \mu_0 d$ and the shunt capacitance $C_R = \varepsilon_0 d$, where d is the periodicity of the unit cell as shown in Fig. 1(a). The cell dimension ($\Delta z = d$) is normally small compared to the wavelength. The series capacitances C_i and the shunt inductances L_i ($i = 1, 2$) are equivalent models for the effect of the LH property. This contributes to the simultaneous exhibition of negative effective permittivity and negative effective permeability, which results in left-handedness behavior. We can directly relate the free-space permittivity and permeability and the per-unit-length capacitance and inductance [11] as given by Equation (2).

The geometry shown in the Fig. 1 can be used to construct the double periodic TL. Assumption is made that the wave is propagating along the z-direction, and independent of the y-direction. In a thin homogeneous isotropic medium, such as microstrip lines, a quasi-static TMx mode wave is considered because of a weak x-variation [11]. The field equations and Helmholtz equation of the TMx mode are given from Maxwell's equations [13] by

$$\begin{cases} E_z = \dfrac{1}{j\omega\varepsilon}\dfrac{\partial H_y}{\partial x} \quad E_x = -\dfrac{1}{j\omega\varepsilon}\dfrac{\partial H_y}{\partial z} \\ \dfrac{\partial^2 H_y}{\partial x^2} + \dfrac{\partial^2 H_y}{\partial z^2} + \omega^2\mu\varepsilon H_y = \dfrac{\partial\varepsilon}{\partial z}\dfrac{\partial H_y}{\varepsilon\partial z} \end{cases} \tag{1}$$

Contributed by the series capacitances and shunt inductances, the

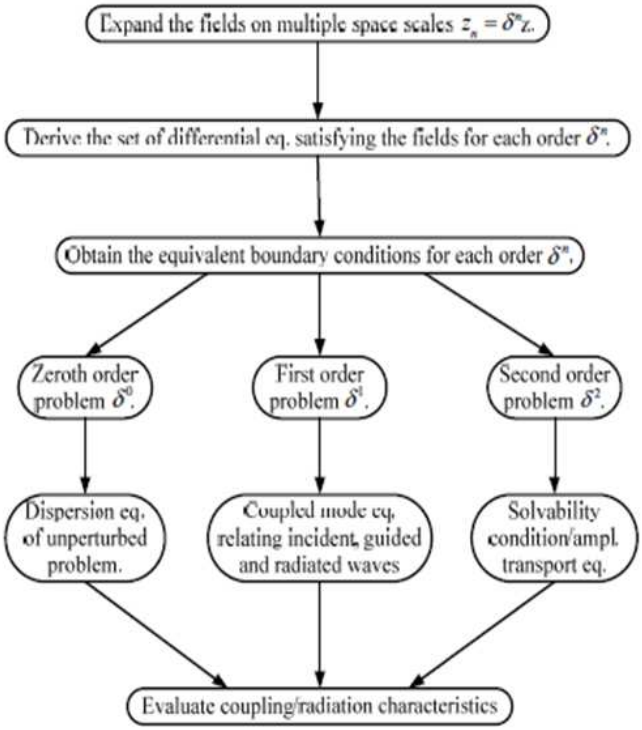

Figure 2. The flow chart of the singular perturbation procedure.

dielectric and magnetic properties consist of a positive contribution due to the host medium and a negative dispersive contribution due to the loaded shunt inductances and series capacitances. The effective permittivity (ε) and permeability (μ) of the material can be given by [11]. These expressions are obtained from Lorentz model.

$$\varepsilon = \varepsilon_0 \varepsilon_{eff} - \frac{1}{\omega^2 L d}, \quad \mu = \mu_0 - \frac{1}{\omega^2 C_0 d} \tag{2}$$

where L and C are the double periodically loaded inductances and capacitances, respectively. The effective permittivity of microstrip lines is [9]

$$\varepsilon_{eff} = \frac{\varepsilon_r + 1}{2} + \frac{\varepsilon_r - 1}{2}\sqrt{\frac{1}{1 + 12h/w}}$$

where h/w is the ratio of height to width of the microstrip line. The Bloch impedance is $Z_B = g\sqrt{\frac{\mu}{\varepsilon}}$ where g is the geometric factor, and

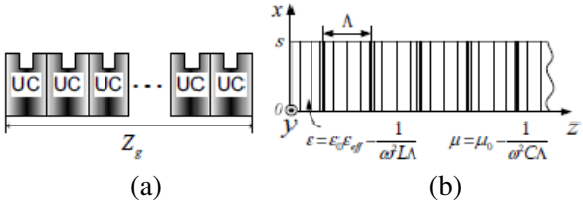

(a) (b)

Figure 3. (a) Layout of the periodic TL. (b) Analytical model of double periodic dielectric on a ground plane.

is dependent on the width and substrate height of the microstrip line. From the expressions, it is noted that the relative permittivity of the host medium is not doubled comparing with the expressions in [11] because of effect of the open-circuited stubs in shunt to the TL is none.

These are the key parameters in the analysis of the double periodic transmission lines. The investigation of the material parameters requires that the series and shunt branches are dominated by C_i and L_i ($i = 1, 2$). The analytical model of the transmission lines investigated is shown in Fig. 3. As previously shown, the effective material permittivity and permeability of the guide are expressed as a function of frequency, periodically loaded capacitances and inductances as shown in (2).

In the double periodic transmission lines, lumped inductances L_i and capacitances C_i are loaded with periodicity 'd', as shown in Fig. 1(a). We consider the transmission line with double periodically loaded both inductances and capacitances. For the transmission line with double periodically loaded inductances and double periodically loaded capacitances, the inductances and capacitances are expanded by

$$\begin{cases} L = L_0\left(1+\delta_L\eta_{L1}\cos(Kz_0+\theta_1)+\delta_L^2\eta_{L2}\cos(2Kz_0+\theta_2)+O\left(\delta_L^3\right)\right) \\ C = C_0\left(1+\delta_C\eta_{C1}\cos(Kz_0+\theta_1)+\delta_C^2\eta_{C2}\cos(2Kz_0+\theta_2)+O\left(\delta_C^3\right)\right) \end{cases} \quad (3)$$

where L_0 is the average inductance, η_{L1} and η_{C1} are the amplitudes of the fundamental (first harmonic) component of the periodically loaded inductance and capacitance respectively, while η_{L2} and η_{C2} are the amplitudes of the second harmonic, δ is a perturbation coefficient smaller than 1, and K is satisfied with Bragg condition $K = 2\pi/d$. The material is assumed to be lossless. The TM mode is considered here with non-vanishing field components H_y, E_x and E_z having no variation in the y-direction. By substituting (3) into (2), a periodically

modulated permittivity profile can be expressed as

$$\begin{aligned}\varepsilon =& \varepsilon_0\varepsilon_{eff} - \frac{1}{\omega^2 L_0 d} + \frac{1}{\omega^2 L_0 d}\delta\eta_1 \cos\left(kz_0+\theta_1\right)\\ &+ \frac{1}{\omega^2 L_0 d}\delta^2\eta_2 \cos\left(2kz_0+\theta_2\right) + O\left(\delta^3\right) \qquad (4a)\\ \frac{\partial\varepsilon}{\partial z} =& \frac{1}{\omega^2 L_0 d}\left(-\delta_L\eta_{L1}k\sin(kz_0+\theta_1) - 2\delta_L^2\eta_{L2}k\sin(2kz_0+\theta_2) + O\left(\delta^3\right)\right)\end{aligned}$$

Including the periodically modulated permeability profile

$$\begin{aligned}\mu =& \mu_0 - \frac{1}{\omega^2 C_0 d} + \frac{1}{\omega^2 C_0 d}\delta_C\eta_{C1}\cos\left(kz_0+\theta_1\right)\\ &+ \frac{1}{\omega^2 L_0 d}\delta_C^2\eta_{C2}\cos\left(2kz_0+\theta_2\right) + O\left(\delta^3\right) \qquad (4b)\end{aligned}$$

The perturbation is carried up to the second-order by introducing space scales in the z-direction as $z_o = z$, $z_2 = \delta^2 z$ with $\frac{\partial}{\partial z_1} = 0$

$$\begin{cases}\dfrac{\partial}{\partial z} = \left(\dfrac{\partial}{\partial z_0} + \delta^2\dfrac{\partial}{\partial z_2}\right)\\ \dfrac{\partial^2}{\partial z^2} = \dfrac{\partial^2}{\partial z_0^2} + 2\delta^2\dfrac{\partial^2}{\partial z_0\partial z_2}\end{cases} \qquad (5)$$

and the expression for H_y is given by

$$\begin{aligned}H_y &= H_{y0} + \delta H_{y1} + \delta^2 H_{y2}\\ \frac{\partial H_y}{\partial z} &= \left(\frac{\partial}{\partial z_0} + \delta^2\frac{\partial}{\partial z_2}\right)\left[H_{y0} + \delta H_{y1} + \delta^2 H_{y2}\right]\\ &= \frac{\partial}{\partial z_0}H_{y0} + \delta\frac{\partial}{\partial z_0}H_{y1} + \delta^2\left(\frac{\partial}{\partial z_2}H_{y0} + \frac{\partial}{\partial z_0}H_{y2}\right)\end{aligned} \qquad (6)$$

where H_{y0}, H_{y1} and H_{y2} are functions of x, z_0 and z_2.

2.1. Zeroth Order of the Problem

The zeroth-order component of H_y inside the substrate satisfies the following differential equation [12]

$$\left\{\frac{\partial^2}{\partial x^2} + \frac{\partial^2}{\partial z_0^2} + \omega^2\mu\varepsilon_{s0}\right\}H_{y0} = 0 \qquad (7)$$

The fields H_{y0} and E_{z0} are continuous at the air-medium interface ($x = s$), and the field $E_{z0} = 0$ at the ground plane ($x = 0$). The

boundary conditions are obtained as

$$\begin{cases} \text{For } x=0\text{: } E_{z0s}=0 \quad \dfrac{\partial H_{y0s}}{\partial x}=0 \\ \text{For } x=s\text{: } H_{y0s}=H_{y0a} \quad E_{z0s}=E_{z0a} \\ \dfrac{1}{\varepsilon_{s0}}\dfrac{\partial}{\partial x}H_{y0s}=\dfrac{1}{\varepsilon_0}\dfrac{\partial}{\partial x}H_{y0a} \end{cases} \tag{8}$$

H_{y0s} and H_{y0a} are the TM mode fields in the medium and free space, respectively.

Based on the differential Equation (7) and the boundary conditions (8), the TM mode field in the medium is satisfied as

$$H_{y0s}=N_g a_g \frac{\cos(k_{xs}x)}{\cos(k_{xs}s)}e^{-jk_z z_0} \tag{9}$$

The TM mode field in the air region is satisfied with Helmholtz Equation (1) and is given by

$$H_{y0a}=N_g a_g e^{-k_{xa}(x-s)}e^{-jk_z z_0} \tag{10}$$

where k_{xa} and k_{xs} are defined from (1):

$$\begin{cases} k_{xa}^2+k_z^2=\omega^2\mu_0\varepsilon_0 & (x>s), \\ k_{xs}^2+k_z^2=\omega^2\mu_{s0}\varepsilon_{s0} & (0<x<s). \end{cases} \tag{11}$$

k_{xa}, k_z, k_{xs} are complex wavenumbers:

$$\begin{aligned} k_{xa} &= k'_{xa}+jk''_{xa}=\beta_{xa}-j\alpha_{xa}; \quad k_{xs}=k'_{xs}+jk''_{xs}=\beta_{xs}-j\alpha_{xs}; \\ k_z &= k'_z+jk''_z=\beta_z-j\alpha_z \end{aligned}$$

By applying the boundary conditions on the air-medium interface $x=s$ and the ground plane $x=0$ (8) to the TM mode fields in the medium and air with (9) and (10), the solution satisfies the relationship as

$$\begin{cases} \dfrac{\partial}{\partial x}H_{y0s}=-N_g a_g k_{xs}\tan(k_{xs}s)\,e^{-jk_z z_0} \\ \dfrac{\partial}{\partial x}H_{y0a}=-N_g a_g k_{xa}e^{-jk_z z_0} \end{cases} \tag{12}$$

The dispersion relation can be obtained from (11) and satisfies

$$k_{xs}\tan(k_{xs}s)=\frac{\varepsilon_{s0}}{\varepsilon_0}k_{xa} \tag{13}$$

The field is a wave of varying amplitude a_g and the unknown normalization constant N_g in (9) and (10) is chosen by considering the power carrier by the guided wave in the z-direction as $|a_g|^2$ over a unit width in the y-direction, where a_g is a guided power along the

transmission line. In the passband, the z component of the attenuation constant of the fundamental harmonic (α_z) is zero. With help of the Poynting power of $|a_g|^2$ toward z-direction, the normalization constant N_g in the passband is obtained as

$$N_g = \left\{ \frac{4\omega\varepsilon_{s0}\beta_{xs}^2\alpha_{xa}}{\beta_z\left[\frac{\varepsilon_{s0}}{\varepsilon_0}\left(\alpha_{xa}^2+\beta_{xs}^2\right)+s\alpha_{xa}\left(\beta_{xs}^2+\frac{s\alpha_{xa}^2{\varepsilon_{s0}}^2}{\varepsilon_0^2}\right)\right]} \right\}^{\frac{1}{2}} \tag{14}$$

2.2. First and Second Order of the Problem

The harmonic variation of the permittivity generates many higher order Floquet modes. For, simplicity, first order Floquet mode is considered along with perturbation orders of δ^1 and δ^2 in first and second order analyses. The corresponding differential equations are given below.

First Order

$$\left\{\frac{\partial^2}{\partial x^2}+\frac{\partial^2}{\partial z_0^2}+\omega^2\mu_{s0}\varepsilon_{s0}\right\}H_{y1}+\frac{\mu_{s0}}{L_0 d}\eta_{L1}\cos\left(Kz_0+\theta_1\right)H_{y0}$$
$$+\frac{\varepsilon_{s0}}{C_0 d}\eta_{C1}\cos\left(Kz_0+\theta_1\right)H_{y0}=-\frac{\eta_{L1}K\sin\left(Kz_0+\theta_1\right)}{\left(\omega^2L_0d\varepsilon_0\varepsilon_{eff}-1\right)}\frac{\partial}{\partial z_0}H_{y0} \tag{15}$$

Second Order

$$\left\{\frac{\partial^2}{\partial x^2}+\frac{\partial^2}{\partial z_0^2}+\omega^2\mu\varepsilon_{s0}\right\}H_{y2}=-2\frac{\partial^2}{\partial z_0\partial z_2}H_{y0}-\frac{\mu_{s0}}{L_0 d}\eta_{L2}\cos(2Kz_0+\theta_2)H_{y0}$$
$$-\frac{\varepsilon_{s0}}{C_0 d}\eta_{C2}\cos(2Kz_0+\theta_2)H_{y0}-\frac{\eta_{L1}\eta_{C1}K\cos(Kz_0+\theta_1)\cos(Kz_0+\theta_1)}{\omega^2L_0C_0d^2}H_{y0}$$
$$-\frac{\eta_{L1}\eta_{C1}K\cos\left(Kz_0+\theta_1\right)\sin\left(Kz_0+\theta_1\right)}{\left(\omega^2L_0d\varepsilon_0\varepsilon_{eff}-1\right)^2}\frac{\partial}{\partial z_0}H_{y0}$$
$$-\frac{2\eta_{L2}K\sin\left(2Kz_0+\theta_2\right)}{\left(\omega^2L_0d\varepsilon_0\varepsilon_{eff}-1\right)}\frac{\partial}{\partial z_0}H_{y0}$$
$$-\frac{\mu_{s0}}{L_0 d}\eta_{L1}\cos\left(Kz_0+\theta_1\right)H_{y1}-\frac{\varepsilon_{s0}}{C_0 d}\eta_{C1}\cos\left(Kz_0+\theta_1\right)H_{y1}$$
$$-\frac{\eta_{L1}K\sin\left(Kz_0+\theta_1\right)}{\left(\omega^2L_0d\varepsilon_0\varepsilon_{eff}-1\right)}\frac{\partial}{\partial z_0}H_{y1} \tag{16}$$

For each order δ^n, the boundary conditions are obtained when the fields H_y and E_z are continuous at $x = s$ and the field $E_z = 0$ at

$x = 0$. Based on the boundary conditions, the solutions of (14) for the first-order is assumed.

$$\begin{cases} H_{y1a} = F_{1a} e^{-\alpha_{1a}(x-s)} e^{-j(k_z+K)} \\ \qquad + N_r a_i e^{j\theta_1} \left(a_i e^{jk_{-1a}(x-s)} + b_i e^{-jk_{-1a}(x-s)} \right) e^{-j(k_z-K)z_0} \\ H_{y1s} = \sum_{i=\pm 1} e^{-j(k_z \pm K)z_0} \left[\dfrac{F_{\pm 1s} \cos(k_{\pm 1s} x)}{\cos(k_{\pm 1s} s)} + \dfrac{G_{\pm 1s} \cos(k_{xs} x)}{\cos(k_{xs} s)} \right] \end{cases} \tag{17}$$

where

$$G_{\pm 1s} = \frac{N_g a_g e^{j\theta_1}}{2(2Kk_z \pm K^2)} \left(\frac{k_z \eta_{L1}}{\omega^2 \varepsilon_0 \varepsilon_{eff} L_0 d - 1} - \frac{\mu_{s0} \eta_{L1}}{L_0 d} - \frac{\varepsilon_{s0} \eta_{C1}}{C_0 d} \right)$$

And

$$\begin{aligned} k_{-1a}^2 &= \omega^2 \mu_0 \varepsilon_0 - (k_z - K)^2 \\ \alpha_{1a}^2 &= -\omega^2 \mu_0 \varepsilon_0 - (k_z + K)^2 \\ k_{\pm 1a}^2 &= \omega^2 \mu_0 \varepsilon_0 - (k_z \pm K)^2 \end{aligned} \tag{18}$$

The first-order solutions contain $k_z - K$ and $(k_z + K)$ terms, which are the wave numbers in z-direction, at least one of the scattered Floquet modes must be a fast wave and then leaky-wave phenomenon occurs. The power flow in the negative x and positive x-directions as incident power $|a_i|^2$ and radiated power $|b_i|^2$, respectively. The normalization factor N_r is evaluated as

$$N_r = \sqrt{\frac{2\omega \varepsilon_0}{k_{-1a}}}$$

The electric fields E_z and E_x can be obtained from Maxwell's equations as (1). Substituting (17) into the boundary conditions of the first-order, F_{-1s}, F_{1s} are obtained. The relation between radiated wave b_i, incident wave a_i and guided wave a_g (as shown in Fig. 4) with in-phase condition $e^{-j(k_z-K)z_0}$ of $\cos(K_x)$ also be derived as [13]

$$b_i = C_{rg} a_g + C_{gg} a_i \tag{19}$$

where

$$C_{rg} = \frac{\begin{array}{l} \dfrac{N_g e^{j\theta_1}}{2(2Kk_z - K^2)} \left(\dfrac{k_z \eta_{L1}}{\omega^2 \varepsilon_0 \varepsilon_{eff} L_0 d - 1} - \dfrac{\mu_{s0} \eta_{L1}}{L_0 d} - \dfrac{\varepsilon_{s0} \eta_{C1}}{C_0 d} \right) \\ (-(-k_{-1s}) \tan(k_{-1s} s) - k_i \tan(k_i s)) \\ - \dfrac{\omega^2 L_0 d \eta_{L1} \cos(Kz_0 + \theta_1)}{2\cos(Kz_0) \left(\omega^2 \varepsilon_0 \varepsilon_{eff} L_0 d - 1\right)^2} N_g (-k_i) \tan(k_i s) \end{array}}{N_r e^{j\theta_1} \left[\dfrac{(-k_{-1s}) \tan(k_{-1s} s)}{\varepsilon_{s0}} + \dfrac{jk_{-1a}}{\varepsilon_0} \right]} \tag{20}$$

$$C_{gg} = -\frac{\varepsilon_0 k_{-1s} \tan(k_{-1s} s) + jk_{-1s} \varepsilon_{s0}}{\varepsilon_0 k_{-1s} \tan(k_{-1s} s) - jk_{-1s} \varepsilon_{s0}}$$

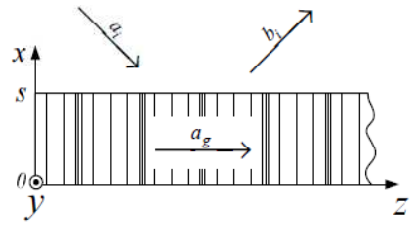

Figure 4. Interaction of the coupling: a_i incident wave, b_i radiated wave, a_g principle guided wave.

where C_{rg} is the coupling coefficient and C_{rr} is the reflection coefficient.

The solutions for the second order are field are assumed as

$$\begin{cases} H_{y2a} = \emptyset_a(x)e^{-jk_z z_0} \\ H_{y2s} = \emptyset_s(x)e^{-jk_z z_0} \end{cases} \tag{21}$$

Substituting the assumed solution and solving the differential equations we get $k_{xa}k_z$ and k_{xs}

$$\begin{cases} \emptyset_a(x) = A_1 e^{-k_{xa}(x-s)} - \dfrac{jk_z}{k_{xa}} N_g \dfrac{da_g}{dz_2} x e^{-k_{xa}(x-s)} \\ \emptyset_s(x) = B_1 \dfrac{\cos k_{xs}x}{\cos k_{xs}s} + C_1 \dfrac{\sin k_{xs}x}{\cos k_{xs}s} + \dfrac{jk_z N_g}{k_{xs}} \dfrac{da_g}{dz_2} \dfrac{x \sin(k_{xs}x)}{\cos(k_{xs}s)} \end{cases} \tag{22}$$

Substituting (21) into the boundary conditions for the second-order at $x = 0$, yield $C_1 = 0$. At $x = s$, followed by the elimination of the arbitrary constants, amplitude transport equation is obtained as

$$\frac{da_g}{dz_2} = C_{gg}a_g + C_{gr}a_i \tag{23}$$

$C_{gg} = C_{ggr} + jC_{ggi}$ is the extinction coefficient. Its real part C_{ggr} gives the leakage coefficient and the imaginary part C_{ggi} determines the exact radiation angle for the optimum radiation efficiency.

In the LWA problem, the incident wave a_i is not considered, since it is based on the scattering of guided waves into a radiated wave due to the presence of a non-uniformity along the waveguide and hence the relations

$$\begin{aligned} b_i &= C_{rg}a_g \\ \frac{da_g}{dz_2} &= C_{gg}a_g \end{aligned} \tag{24}$$

In a finite length Z_g of the permittivity modulated TL, the radiation efficiency Q_0 and radiation angle θ_r of the leaky wave radiating from

the TL with double periodically loaded inductances and capacitances can be obtained from

$$Q_0 = \frac{\int_0^{Z_g} |b_i|^2 \, dz_2}{|a_g|^2_{z_2=0}} = 1 - e^{2C_{ggr}Z_g} \tag{25}$$

$$\theta_r = \tan^{-1}\left(\frac{k_{-1a}}{\beta - K - C_{ggi}}\right)$$

where Z_g is the total length of the periodic TL. The radiation efficiency is defined as the ratio of the total power radiated from the modulated region to the guided wave power incident at $z_2 = 0$ [13].

3. NUMERICAL RESULTS

It is assumed that the thickness of the TL $s = 1.6\,\text{mm}$, the average loaded inductance $L_0 = 5.05\,\text{nH}$, the loaded capacitance $C_0 = 0.5\,\text{pF}$, periodicity of the loaded elements is $d = 10\,\text{mm}$, relative permittivity of the substrate $\varepsilon_r = 4.5$, and it is considered as non-magnetic. We can calculate the phase constant of the fundamental space harmonic, only when we assume the periodic permittivity modulation applied is same as the unperturbed phase constant. When $k_{xs} \neq 0$, we need to consider Quasistate TM mode solution.

Dispersion Diagram aids a better understanding of left Handed and the right Handed regions of the given structure. In Fig. 5, we can see the dispersion diagram of the proposed Double periodic TL. We

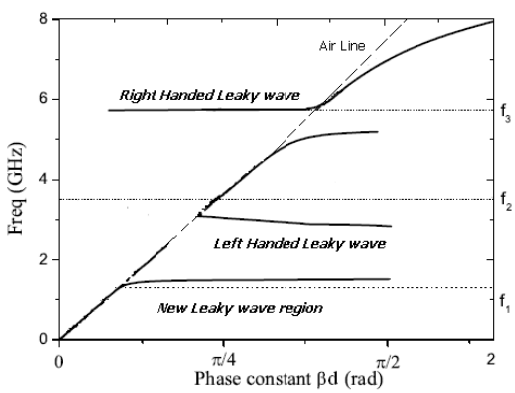

Figure 5. Dispersion characteristics of the double periodic TL based on singular perturbation procedure, quasi-static TM mode.

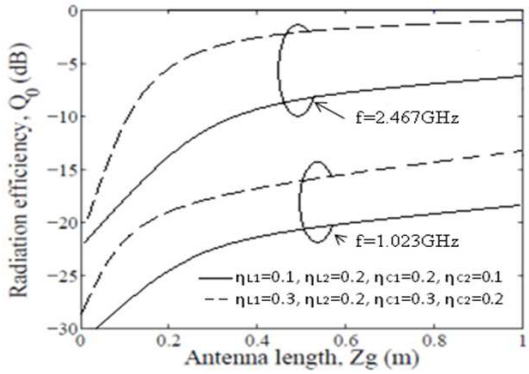

Figure 6. Radiation efficiency as a function of antenna length for different modulation indices.

can identify three main regions: (1) New Leaky wave region, (2) Left Handed Passband (3) Right Handed Passband. The frequencies at which these properties are displayed are $f_1 = 1.023\,\text{GHz}$, $f_2 = 2.467\,\text{GHz}$ and $f_3 = 4.567\,\text{GHz}$ respectively. The curves at f_1, f_2 and f_3 are inside the airline boundary ($\beta = \omega\sqrt{\mu_0\varepsilon_0}$). In addition to the fact that the proposed antenna radiates both backward and forward at frequencies f_2 and f_3 respectively, it can radiate a forward wave at $f_{leaky} = f_1$ which is below the LH passband.

The bandwidth of the stopband is comparatively wider than in the case of single periodic TL [1]. In both right handed (RH) and LH passband, the phase constant of the double periodic TL approaches that of single periodic.

From the Single Periodic Method we also obtain the radiation efficiency Q_0. We have obtained the radiation efficiency at around frequencies f_1 and f_2. We have four parameters which play an important role in deciding the radiation efficiency viz. η_{L1}, η_{C1}, η_{L2} and η_{C2}. The values of the modulation index have been suitable chosen so as to give better efficiency. The two combinations of values chosen are $\eta_{L1} = 0.1$, $\eta_{C1} = 0.2$, $\eta_{L2} = 0.2$, $\eta_{C2} = 0.1$ and $\eta_{L1} = 0.3$, $\eta_{C1} = 0.3$, $\eta_{L2} = 0.2$, $\eta_{C2} = 0.2$. The radiation efficiency Q_0 of (27) is numerically estimated around the new right-handed leaky-wave region ($f_{leaky} = f_1$) and the LH leaky-wave region ($f = f_2$) as a function of TL length Z_g as shown in Fig. 6. It can be seen from Fig. 6 that the radiation efficiency for the new leaky-wave right-handed region is smaller than the radiation behavior in the LH region. It may be developed for large η values from 0.1 up to 0.3 beyond which it exceeds the limit of singular perturbation procedure [12]. It is noted that the

radiation efficiency at $f_{leaky} = f_1$ is less than that at $f = f_2$ and longer transmission lines are needed to get more radiation efficiency.

4. REALIZATION

The proposed structure has been realized in a double periodic manner with both inductance and the capacitance modulated along the propagation axis. The structure has been implemented on a microstrip line. The periodicity for the given structure (d) is 10 mm with eight unit cells. The dimensions of the structure follow the single perturbation analysis and they can be referred from fig. The width of the microstrip line is 3.7 mm and the thickness is 1.6 mm. The proposed structure is implemented on a FR-4 substrate with relative dielectric constant $\varepsilon_r = 4.5$.

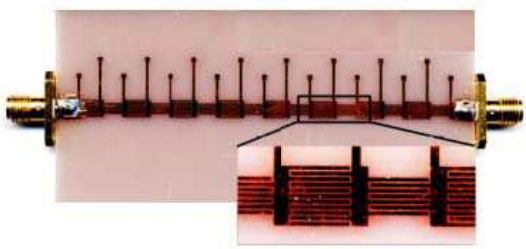

Figure 7. Fabricated proposed double periodic TL structure.

Figure 7 shows the fabricated prototype of the proposed double periodic CRLH TL. It can be seen that the inductance that has been realized as a stub with a via, and the capacitance which has been realized as gap between interdigited fingers which is shown in Fig. 1, have both been varied in length in a double periodic fashion. We can see the simulated and measured scattering parameters of the TL in Fig. 8. The frequency responses of the double periodic TL which is predicted by the singular perturbation method (SPM) can be seen exhibiting a new leaky wave phenomenon. The measurements have been made using Agilent N5230 PNA-L Network Analyzer.

It has been experimentally verified [1] that no leaky wave property in the LH passband can be found in the single periodic CRLH TL. This highlights the fact that double periodic TL has an advantage over single periodic TL in terms of leaky wave radiation in the given frequency range. Fig. 8 also shows the double periodic composite right/left handed (DP CRLH) group delay.

The far-field radiation patterns of the proposed antenna designed

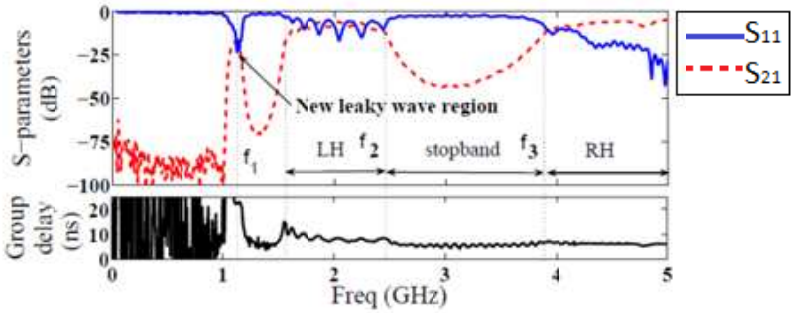

Figure 8. Measured frequency responses of TLs.

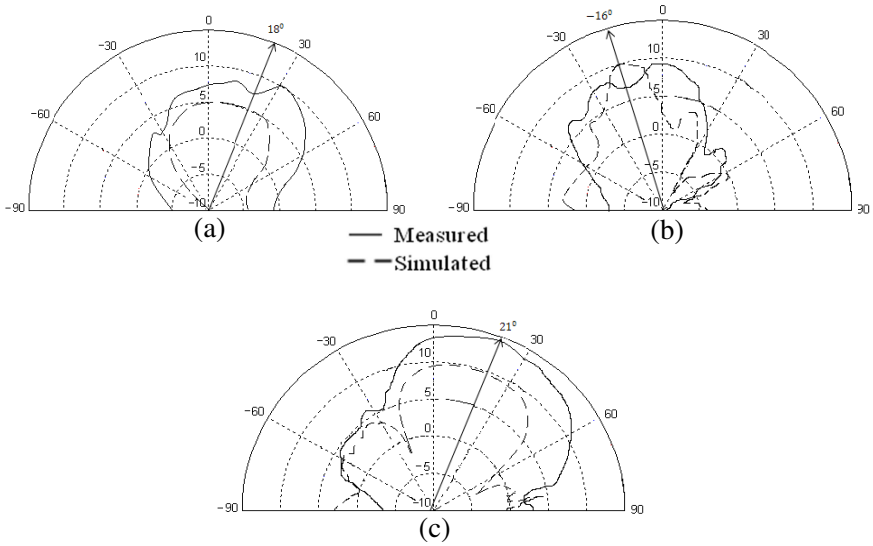

Figure 9. Measurement E-field radiation patterns in decibel scale at measured at (a) $f_1 = 1.023\,\text{GHz}$, (b) $f_2 = 2.467\,\text{GHz}$ and (c) $f_3 = 4.567\,\text{GHz}$.

using microstrip line double periodically loaded with both series interdigital capacitances and shunt inductances are measured at $f_1 = 1.023\,\text{GHz}$ (new leaky wave, forward radiation), $f_2 = 2.467\,\text{GHz}$ (LH, backward radiation) and $f_3 = 4.567\,\text{GHz}$ (conventional RH, forward radiation) as shown in Fig. 9. Both the simulated and measured results have been shown. The theoretical farfield pattern has been obtained from Eq. (25). The experimental discrepancies arise because

of soldering errors, shorting of interdigital gap if not etched properly etc.

5. CONCLUSION

We have proposed a double periodic TL structure with both inductance and capacitance loaded. Single perturbation method has been employed to analyze the proposed CRLH structure. Numerical Expressions have been obtained which aid in obtaining dispersion characteristics, propagation constant and radiation characteristics. We have also included the modulation of the permittivity which has increased the degree of freedom of the analysis. The radiation efficiency has been plotted as a function of antennas length to illustrate the effect of modulating indices on the antenna performance. It has been obtained at the three frequencies of interest. We also observe a novel leaky wave region with narrow bandwidth.

REFERENCES

1. Itoh, T. and C. Caloz, *Electromagnetic Metamaterials: Transmission Line Theory and Microwave Applications*, John Wiley Press, 2006.
2. Gupta, K. C., R. Garg, and I. Bahl, *Microstrip Lines and Slotlines*, Artech House, Inc. Press, 1996.
3. Jin, C., A. Alphones, and M. Tsutsumi, "Leaky-wave characteristics from double periodic composite right/left handed transmission lines," *IET Microwaves, Antennas & Propagation*, Vol. 5, No. 12, 1399–1407, 2011.
4. Jin, C., A. Alphones, and L. C. Ong, "Broadband leaky-wave antenna based on composite right/left handed substrate integrated waveguide," *Electronics Letters*, Vol. 46, 1584–1585, 2010.
5. Tsutsumi, M., C. Jin, and A. Alphones, "Leaky wave phenomenon from double periodic left handed waveguide," *Proc. Int. Conf. Asia-Pacific Microwave Conferance*, 1238–1241, Singapore, Dec. 2009.
6. Park, W. S. and S. R. Seshadri, "Theory of the grating coupler for a grounded-dielectric-slab waveguide," *IET Proc. Microwave Antennas Propag.*, Vol. 132, 149–156, 1985.
7. Caloz, C. and T. Itoh, "Transmission line approach of left-handed (LH) materials and microstrip implementation of an artificial LH transmission line," *IEEE Trans. Antennas and Propagation*, Vol. 52, 1159–1166, 2004.

8. Aznar, F., M. Gil, J. Bonache, and F. Martin, "Revising the equivalent circuit models of resonant-type metamaterial transmission lines," *Proc. Int. Conf. IEEE MTT-S International Microwave Symposium Digest*, 322–325, Atlanta, GA, Sep. 2008.
9. Pozar, D., *Microwave Engineering*, John Wiley Press, 1998.
10. Gupta, K. C., R. Garg, and I. Bahl, *Microstrip Lines and Slotlines*, Artech House, Inc. Press, 1996.
11. Eleftheriades, G. V., A. K. Iyer, and P. C. Kremer, "Planar negative refractive index media using periodically L-C loaded transmission lines," *IEEE Trans. Microw. Theory Tech.*, Vol. 50, 2702–2712, 2002.
12. Mark, H. H., *Introduction to Perturbation Methods*, Springer-Verlag Press, 1995.
13. Alphones, A. and M. Tsutsumi, "Leaky-wave radiation from a periodically photoexcited semiconductor slab waveguide," *IEEE Trans. Microw. Theory Tech.*, Vol. 43, 2435–2441, 1995.
14. Pendry, J. B., A. J. Holden, D. J. Robbins, and W. J. Stewart, "Magnetism from conductors and enhanced nonlinear phenomena," *IEEE Trans. Microw. Theory Tech.*, Vol. 47, 2075–2084, 1999.
15. Tsutsumi, M., "Negative refractive index transmission media and its applications to the microwave circuits," *Journal of IEICE*, Vol. 88, 23–27, 2005.
16. Eleftheriades, G. V. and K. G. Balmain, *Negative-refraction Metamaterials: Fundamental Principles and Applications*, John Wiley Press, 2005.